



OPEN

Synthesis of divanillic acid-based aromatic polyamides with linear and branched side-chains and the effect of side-chain structure on thermal and mechanical properties

Yukiko Enomoto , Yuto Amanokura, Kazuma Yagura & Tadahisa Iwata

Divanillic acid (DVA)-based aromatic polyamides (PAs) consisting of DVA with linear (methyl, butyl, hexyl, and octyl groups) or branched (isopropyl and isobutyl groups) side chains and 4,4'-methyl dianillin were synthesized as high-performance and ultra-high-performance biomass plastics. The DVA PAs were amorphous with high thermal stability (decomposition temperature of ca. 380 °C). The glass transition temperature (T_g) of the DVA PAs depended on the side-chain composition in a linear manner, indicating the PA main chain possessed a random structure. The polymers were pressed to form melt-pressed films. The DVA PAs with a higher content of shorter side chains exhibited both higher T_g and tensile strength than those of polymers with a lower content of shorter side chains. The PAs exhibited T_g in the range of ca. 150–253 °C. The branched PA with isopropyl side chains exhibited the highest T_g of 253 °C and highest tensile strength of 63 MPa among the DVA PAs. The PAs with isopropyl side chains and some linear side chains (methyl/hexyl combination) exhibited high tensile strength of approximately 60–70 MPa; however, their T_g varied from 170 to 253 °C. The branched PA exhibited the highest T_g , tensile strength, and Young's modulus of the polymers. The thermal stability and mechanical properties of the PAs were tuned by their side-chain structure and composition.

Keywords Divanillic acid, Aromatic polyamide, Ultra-high-performance plastic, Biomass plastic, Film

There are growing concerns over petroleum depletion, climate change, and plastic waste pollution. As a contributing solution to these problems, bioplastics produced from renewable resources have been receiving increasing attention. Various bio-based compounds that are candidate monomers for bioplastics can be obtained from lignocellulose or other bio-based materials^{1,2}. However, currently developed commercial bioplastics, such as bio-polyethylene, bio-polyethylene terephthalate (bio-PET), poly(butylene succinate), and poly(lactic acid), are mostly targeting to replace common plastics. Common plastics account for around 70% of plastics, have relatively low thermal stability and/or mechanical strength, and are used generally at ambient temperature for packaging or containers. The remaining about 30% of plastics include high-performance plastics, ultra-high-performance plastics, and thermosets, which have superior properties to common plastics, such as high thermal stability, mechanical strength, durability, and chemical resistance. In particular, there has been growing demand for high-performance and ultrahigh-performance plastics in the fields of automobiles, medical science, and electronic devices. Conventional petroleum-based plastics that are categorized as ultra-high-performance plastics, such as aromatic polyamides (PAs; e.g., Aramide® and Kevlar®), polyimides, and polyetheretherketones, are known to exhibit specifically high thermal and mechanical properties. Such properties originate from the rigid aromatic structure of the main chain and polar, rigid bonding structure. Considering the growing demand for these high-performance plastics and that considerable amounts of these plastics are produced from petroleum, it is essential to replace these plastics with bio-based materials to decrease petroleum consumption and carbon dioxide emissions.

Science of Polymeric Materials, Department of Biomaterial Sciences, Graduate School of Agricultural and Life Sciences, The University of Tokyo, 1-1-1 Yayoi, Bunkyo-ku, Tokyo 113-8657, Japan. ✉email: enomotoyukiko@g.ecc.u-tokyo.ac.jp

Bio-based terephthalic acid and 2,5-furandicarboxylic acid (FDCA), which can be obtained from glucose, are most promising monomers for bioplastics. At present, bio-PET and polyethylene furandicarboxylate are successful examples of high-performance biomass plastics^{3,4}. Bio-based aromatic polymers derived from FDCA^{5,6}, 4-amino-cinnamic acid^{7,8}, and 3-amino-4-hydroxybenzoic acid⁹ have been reported to exhibit high thermal stability and favorable mechanical properties. However, the variety of bio-based alternatives to cover a wide range of the properties of petroleum-based high-performance plastics, particularly ultra-high-performance plastics, is currently limited.

Vanillin and its derivatives are attractive aromatic compounds because of their potential for industrial mass production through the decomposition of lignin, which is abundant in plants². Vanillin has a simple structure with carbonyl and phenol groups on the aromatic ring, so many vanillin-derived polymers have been synthesized^{10–15}. However, despite much work on the synthesis of vanillin-based polymers, their use as plastic materials, e.g., in film preparation, has not been sufficiently investigated because of the difficulty of obtaining high-molecular-weight polymers and their low solubility and/or processability.

Divanillic acid (DVA) can be obtained *via* simple dimerization of vanillic acid by enzymatic oxidation. DVA can improve the reactivity of vanillin-based monomers during polymerization and increase the molecular weight of the obtained polymers^{16–18}. Recently, we have synthesized a variety of DVA-derived polymers such as polyesters^{19–23}, PAs^{24,25}, polyketones²⁶, and vitrimers²⁷ with different alkyl side-chain lengths to improve their processability. The thermal processability of these polymers was increased by the alkyl side chain of the DVA unit, and some of these polymers formed self-standing thermo-pressed films. In particular, DVA PAs had extremely high glass transition temperatures (T_g) ranging from 260 to 320 °C^{24,25}. The DVA PA films also exhibited high mechanical strength (ca. 60 MPa). Such properties make DVA PAs promising as bio-based ultrahigh-performance plastics. However, the thermal stability, thermal processability, and mechanical strength of these materials showed a trade-off relationship. The films with higher T_g were sometimes rigid and brittle, and those with good processability and high mechanical strength had relatively lower T_g , although it was still above 200 °C. The range over which the thermal and mechanical properties of these polymers could be controlled was insufficient to make these PAs suitable for a wide range of applications.

In the previous study by our research group, we have synthesized various polysaccharide ester derivatives with various alkyl side-chains as novel bio-based plastics. We have been reported and proposed that combination of alkyl esters with different compositions are effective method to control their thermal and mechanical properties^{28–32}. In particular, polysaccharide esters with branched alkyl side-chains exhibited extraordinary higher thermal properties compared to linear polysaccharide esters^{29–32}. Therefore, in the present study, we have applied the same strategy to the bio-based aromatic polymers on the assumption that combination of side-chains and introduction of branched side-chains might work to control and improve the properties of bio-based PAs.

In the present study, to improve and optimize both the thermal and mechanical properties of DVA-based PAs, we synthesize a variety of PAs with different combinations of alkyl side chains and branched side chains. The effects of the chemical structure and composition of side chains on the thermal and mechanical properties of DVA PAs are explored.

Results and discussion

Synthesis and characterization of DVA PAs

DVA PAs with branched side chains and different combinations of four side-chain structures were synthesized by polycondensation of DVA monomers and MDA, as shown in Fig. 1. MDA was selected as a comonomer because it has a relatively flexible structure and reported DVA PAs with MDA exhibited relatively higher processability and mechanical strength than those of other aromatic diamines²⁴. The conditions used to synthesize the PAs are listed in Table 1. The PAs were white or gray in color and formed as a solid block or powder. The reactivity of the DVA monomers in polycondensation to form linear PAs was not hindered by the presence of a branched or long alkyl side-chain structure.

M_n , M_w , and M_w/M_n of the PAs were measured by SEC; the results are listed in Table 1. Representative SEC curves of PAs are given in Fig. 2. The relatively low M_w/M_n values (< 2.0) of the PAs were ascribed to fractionation during the reprecipitation process. The M_w values of the PAs ranged from approximately 7.0×10^4 to 25×10^4 g mol⁻¹. It seemed that M_w tended to be relatively higher when side-chain is shorter. Investigation of the solubility of DVA PAs in organic solvents revealed that the samples dissolved well in polar aprotic solvents such as NMP, dimethyl sulfoxide, DMAc, and dimethyl formamide at room temperature at a concentration of ca. 20 mg/mL, but did not dissolve in chloroform, ethanol, methanol, or ethyl acetate under the same conditions.

The chemical structures of the PAs were determined by ¹H and ¹³C-NMR spectroscopy, as shown in Fig. 3. All proton peaks derived from DVA and side-chain units were assigned. The proton signal at approximately 10.5 ppm, assigned to amide (NH) protons, was observed for all PAs, which indicated that the desired PAs had been synthesized. The methoxy groups (CH₃O) of the DVA units, and the CH₃ and CH₂ peaks of the butyl and hexyl groups of side chains were all assigned (Fig. 3ab). The compositions of side-chains were calculated based on the ratio of the peak areas of CH₃ protons of different side-chains. The CH₃ and CH peaks of isopropyl groups were clearly observed, as shown in Fig. 3c. The carbon peaks of methoxy and other side-chains, the aromatic carbons, and the carbonyl carbons were also assigned as shown in Fig. 3d-f. It was difficult to discuss specific sequence of DVA units of the copolyamides from these spectra, therefore it seemed that the PA had random sequence.

Thermal properties of DVA PAs

The thermal characteristics of the PAs were investigated by TGA and DMA. The resultant decomposition temperatures—1% weight loss ($T_{d1\%}$) and 5% weight loss ($T_{d5\%}$)—and T_g values are listed in Table 2.

The TGA curves of the PAs are shown in Fig. 4. The $T_{d1\%}$ and $T_{d5\%}$ values of all PAs were in the ranges of approximately 220–300 °C and 350–395 °C, respectively, and were almost independent of the side-chain length

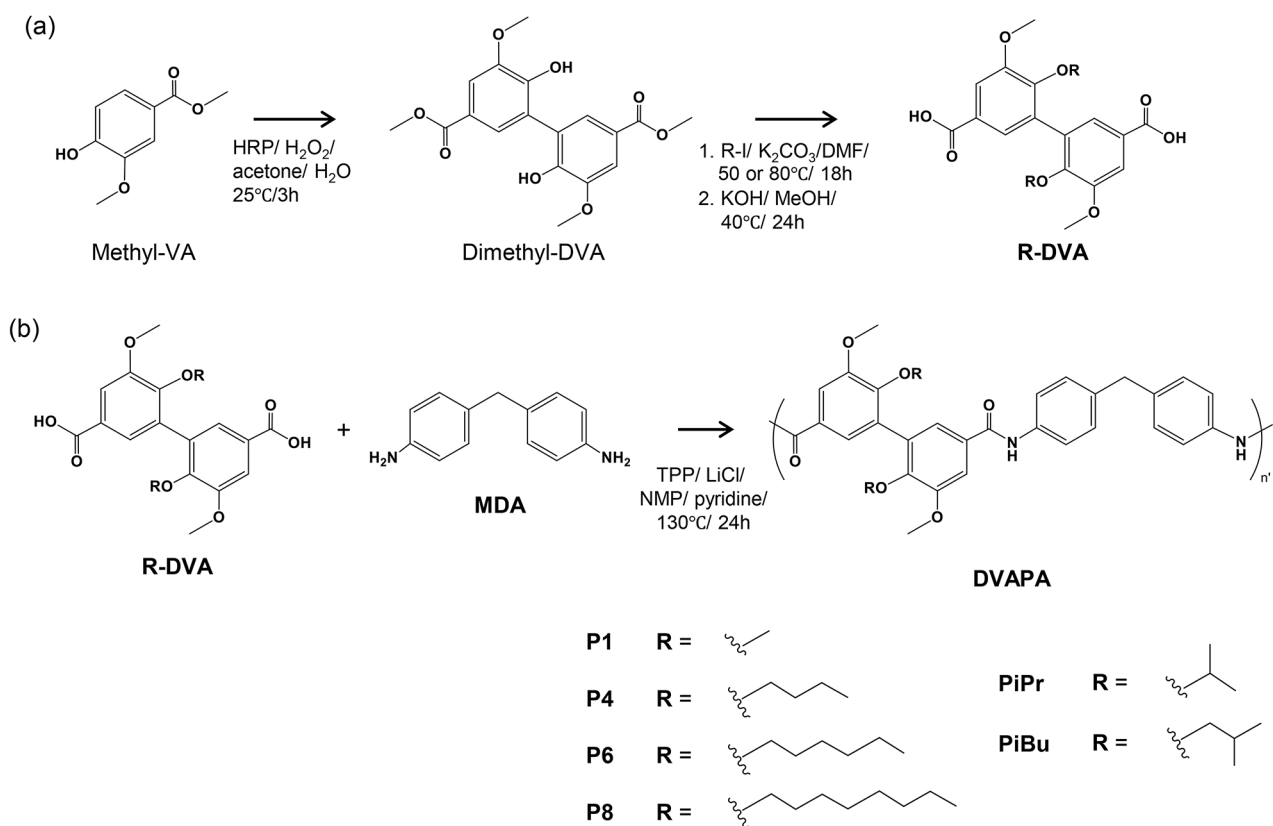


Fig. 1. Synthetic scheme of (a) DVA monomers and (b) DVA PAs.

Polyamides	Side-chain alkyl carbon number	Side-chain composition (mol %)		Short-chain monomer (mg)	Long-chain monomer (mg)	Yield (%)	M_n^b (10^4 g/mol)	M_w^b (10^4 g/mol)	M_w/M_n^b	
		In feed	Calculated ^a							
P1	1	100	100	333	-	85.3	10.8	15.0	1.4	
P4	4	100	100	442	-	75.8	15.3	21.1	1.4	
P6	6	100	100	500	-	81.3	11.7	16.6	1.4	
P8	8	100	100	557	-	88.3	10.5	15.0	1.4	
P16-	75/25	1,6	75/25	77/23	272	125	79.9	15.9	25.0	1.6
	50/50	1,6	50/50	54/46	236	563	43.9	6.9	8.7	1.3
	25/75	1,6	25/75	23/77	83	376	88.9	6.3	7.7	1.2
P18-	75/25	1,8	75/25	72/28	272	139	81.6	9.7	13.0	1.3
	50/50	1,8	50/50	73/27	166	278	68.4	5.8	7.0	1.2
P18-	25/75	1,8	25/75	35/65	84	418	73.8	6.7	8.4	1.3
	75/25	4,6	75/25	76/24	334	125	81.6	14.2	19.6	1.4
P46-	50/50	4,6	50/50	50/50	222	250	77.7	14.4	20.1	1.4
	25/75	4,6	25/75	23/77	112	376	76.1	8.7	11.1	1.3
PiPr	3 (branched)	100	100	1200	-	84.6	7.6	13.1	1.7	
PiBu	4 (branched)	100	100	1200	-	85.8	5.6	9.3	1.7	

Table 1. Synthetic conditions and molecular weights of DVA PAs.

and structure. All PAs exhibited high resistance to thermal decomposition. The $T_{d10\%}$ of P1 (239 °C) was lower than the T_g (278 °C). This weight loss could have been due to the loss of traces of solvent or moisture. It was difficult to remove the unknown residue and dry the sample completely. After DMA, the amount of the residue remaining as char was approximately 60% in weight; it is likely that this is composed of non-volatile aromatic components.

Differential scanning calorimetry (DSC) was also performed to investigate the thermal properties of PAs. The absence of peaks derived from crystal melting indicates that all DVA PAs were amorphous polymers, as

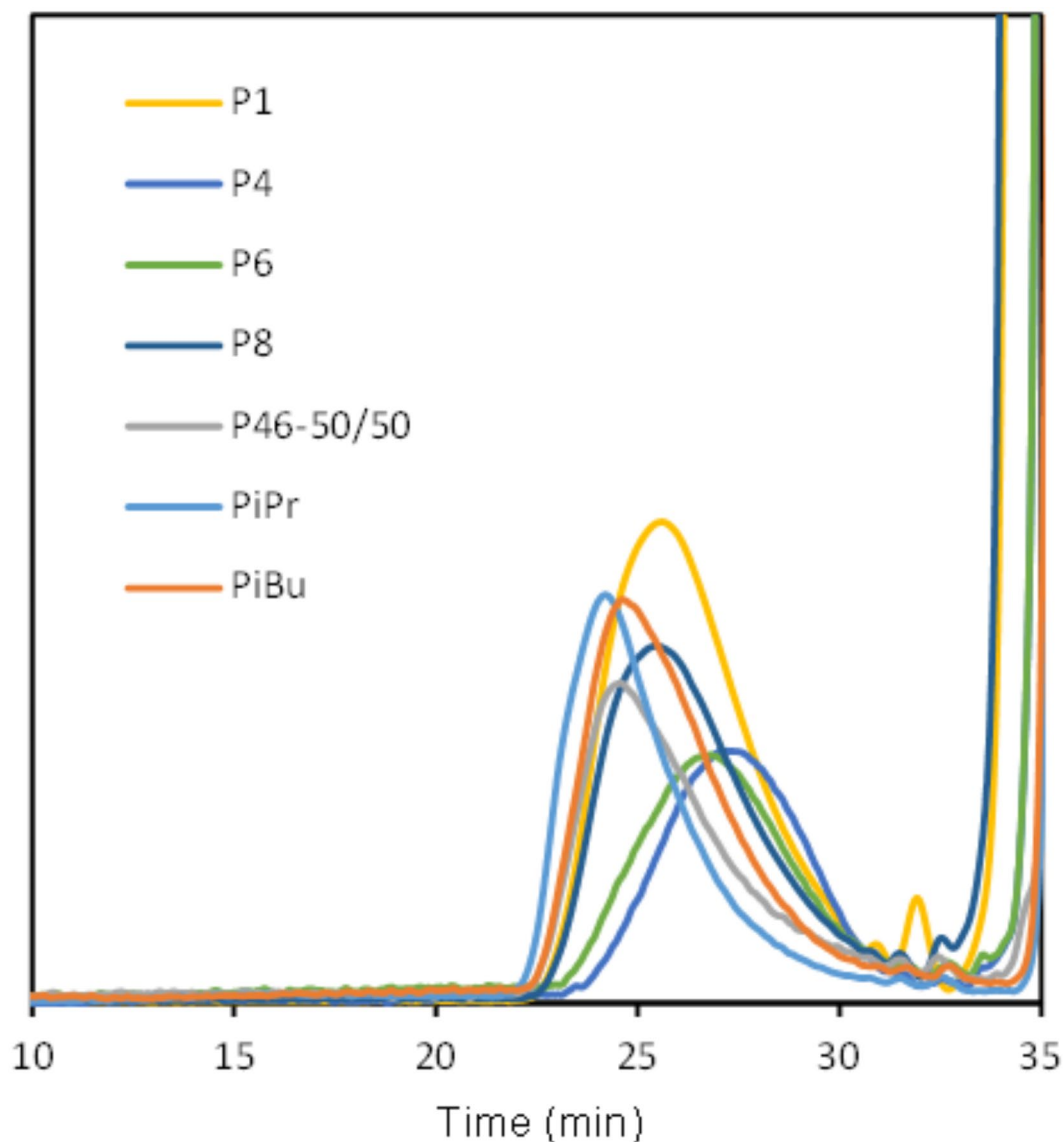


Fig. 2. Representative SEC elution curves of DVA PAs.

discussed in previous studies^{24,25}. Glass transitions were not clearly observed in DSC curves, so T_g values could not be determined by DSC.

The T_g values of the PAs were determined from the peak temperatures of $\tan \delta$ in corresponding DMA curves, as shown in Fig. 5. In a previous study, the T_g values of DVA PAs with shorter side chains tended to be higher than those of DVA PAs with longer side chains²⁴. In the case of the co-PAs with different composition ratios of linear side chains, the T_g values strongly depended on the composition ratio of the side chains. The variation of T_g arises from the effects of side-chain length on the flexibility of the polymer backbone and strength of intermolecular bonding. Figure 6 shows plots of T_g against the ratio of short to long side chains (i.e., composition ratio). The T_g values depended on the composition ratio in an approximately linear manner. The theoretical values of T_g of the copolymers were calculated using the Fox equation ($T_g = w_A T_{gA} + w_B T_{gB}$)^{33–35}, as indicated by dotted lines in Fig. 6. However, w_A and w_B are the compositions of monomer A and B, respectively, and T_{gA} and T_{gB} are the glass transition temperatures of polymer A and B, respectively. The experimental T_g values almost coincided with the theoretical values, indicating that these PAs are random copolymers and that DVA monomers were incorporated quantitatively into the polymer main chain regardless of side-chain structure.

The T_g values of PAs with branched side chains, namely PiPr and PiBu, were 253 and 235 °C, respectively, which were higher than those of PAs with linear side chains, indicating that the introduction of branched side chains led to increased thermal stability. Except for P1 with the shortest side chain and a T_g of 278 °C, PiPr exhibited the highest T_g of 253 °C. In the case of the PAs with branched side chains, PiPr exhibited a higher T_g than that of PiBu, which is probably because PiPr has shorter alkyl side chains than PiBu. Similar phenomena have been observed in the case of polysaccharide ester derivatives with branched side-chains which exhibited extraordinarily higher T_g and T_m compared to the esters with linear side-chains and the polymer with iPr side-

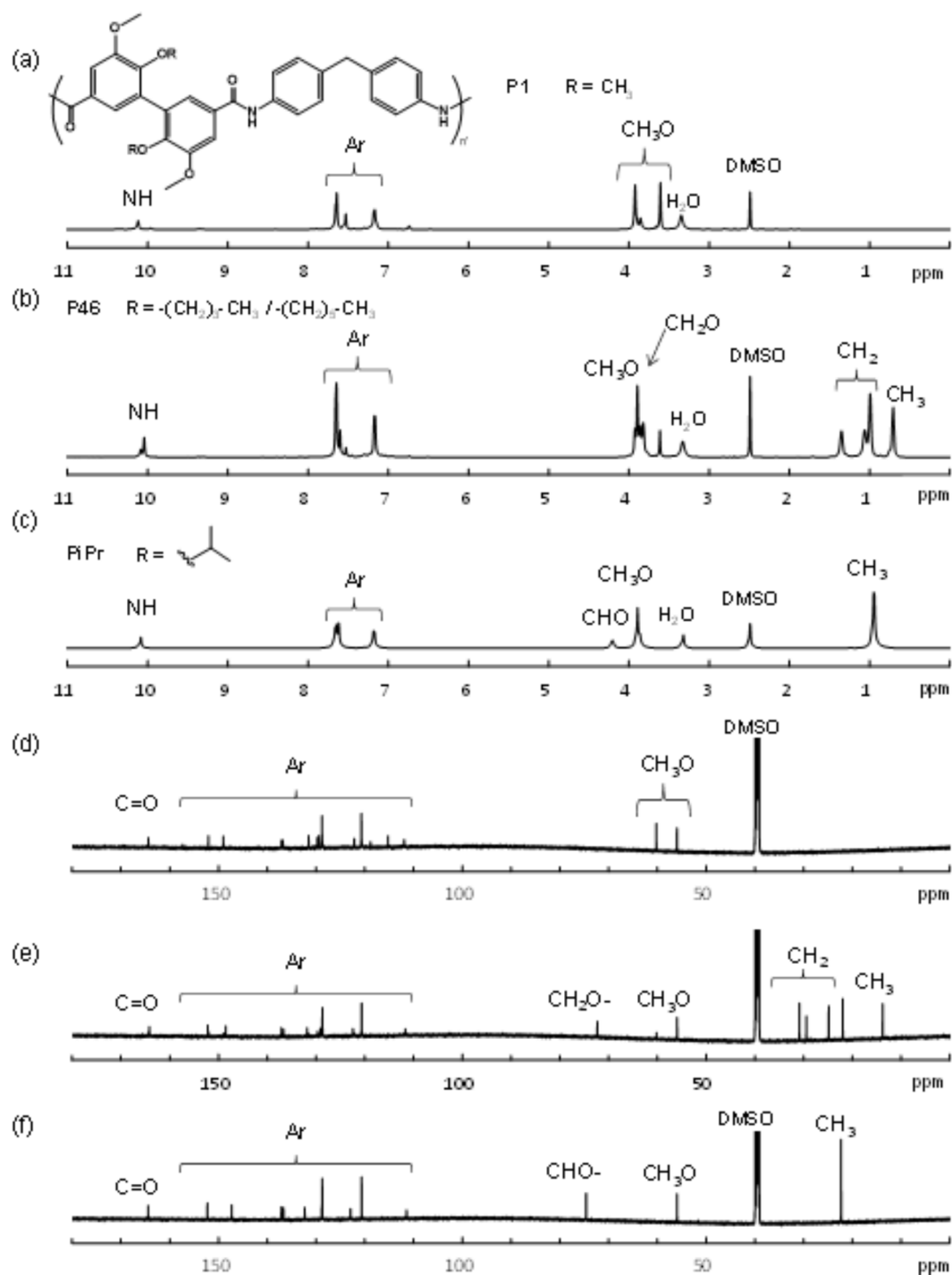


Fig. 3. ^1H - and ^{13}C -NMR spectra of (a) (d) P1, (b) (e) P46-25/75 and (c) (f) PiPr. $\text{DMSO-}d_6$ as solvent.

chains exhibited higher T_g than the polymer with iBu side-chains^{29–32}. Generally, petroleum-based plastics or aromatic polymers have no side-chains. To our knowledge, it was difficult to find similar studies on the other plastics or polymers with branched side-chains. The phenomena might be caused by molecular mobility limitation owing to the introduced branched side-chains as discussed in the previous study.

Film preparation and properties

Figure 7 shows photographs of the thermo-pressed films of DVA PAs pressed at 240 to 300 °C. The processing temperature was determined based on DMA analyses, which indicate T_g of the PAs. The films were almost uniform in color and thickness. The stress–strain curves of the thermo-pressed films of DVA PAs are presented in Fig. 8. The tensile strength, Young's modulus, and elongation at break of the films are listed in Table 3. Figure 9 plots the mechanical strength and T_g of the thermo-pressed films. Some of the thermo-pressed films were too

Polyamides	$T_{d1\%}$ (°C)	$T_{d5\%}$ (°C)	T_g (°C) ^a
P1	239	357	278
P4	242	372	201
P6	331	395	170
P8	161	384	157
P16-75/25	258	376	225
P16-50/50	231	375	211
P16-25/75	221	374	179
P18-75/25	248	358	220
P18-50/50	236	338	202
P18-25/75	247	368	170
P46-75/25	298	379	201
P46-50/50	290	385	198
P46-25/75	301	381	170
PiPr	299	351	253
PiBu	289	383	235

Table 2. Thermal properties of DVAPAs. ^aDetermined by DMA.

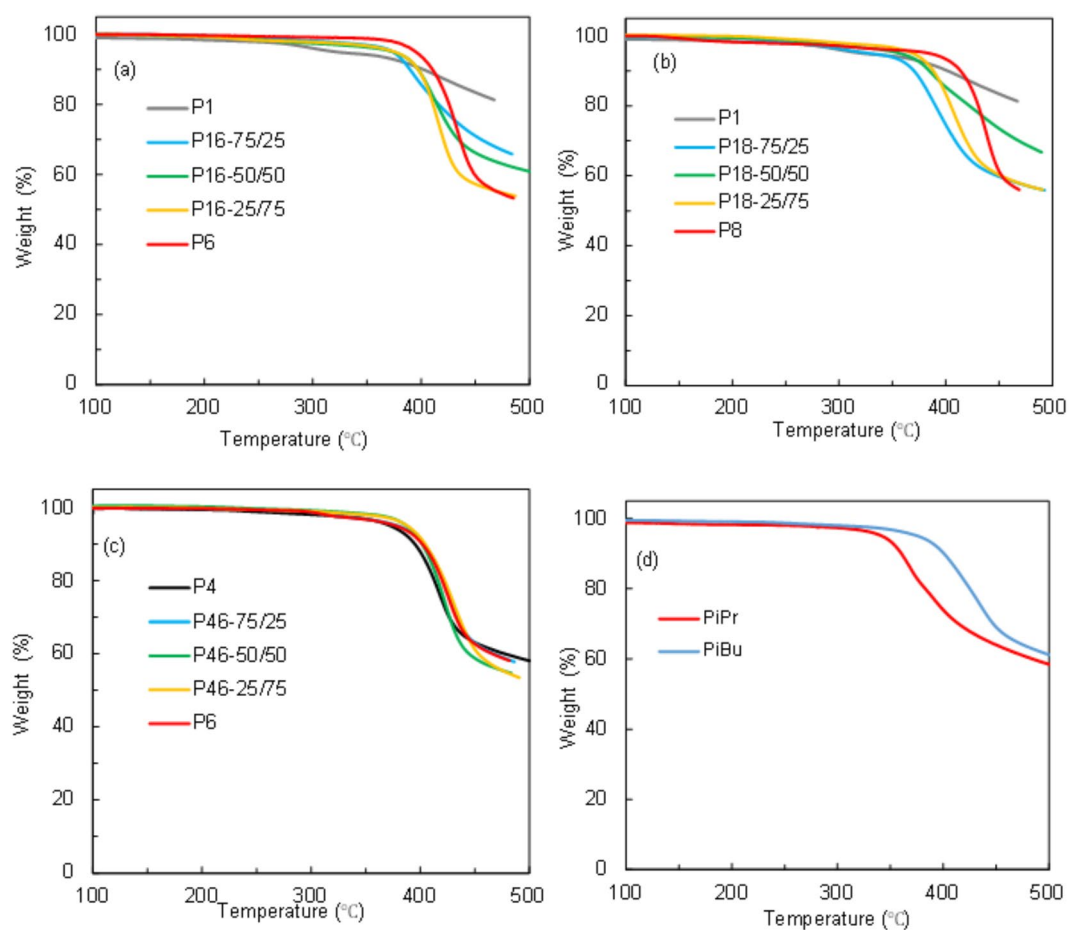


Fig. 4. TGA thermograms of (a) P16, (b) P18, (c) P46, and (d) branched DVAPAs.

hard to prepare specimens for tensile testing. The side-chain length and stiffness of the monomers affected the strength of the intermolecular bonds, which influenced the mechanical properties of DVA-derived polyesters and PAs. In the case of the PAs with methyl (number of carbon atoms $n = 1$), butyl ($n = 4$), hexyl ($n = 6$), and octyl ($n = 8$) side chains, that is, P1, P4, P6, and P8, respectively, it was expected that the PAs with shorter side chains would be harder and stronger and the PAs with longer side chains would be softer and weaker. As expected, P1

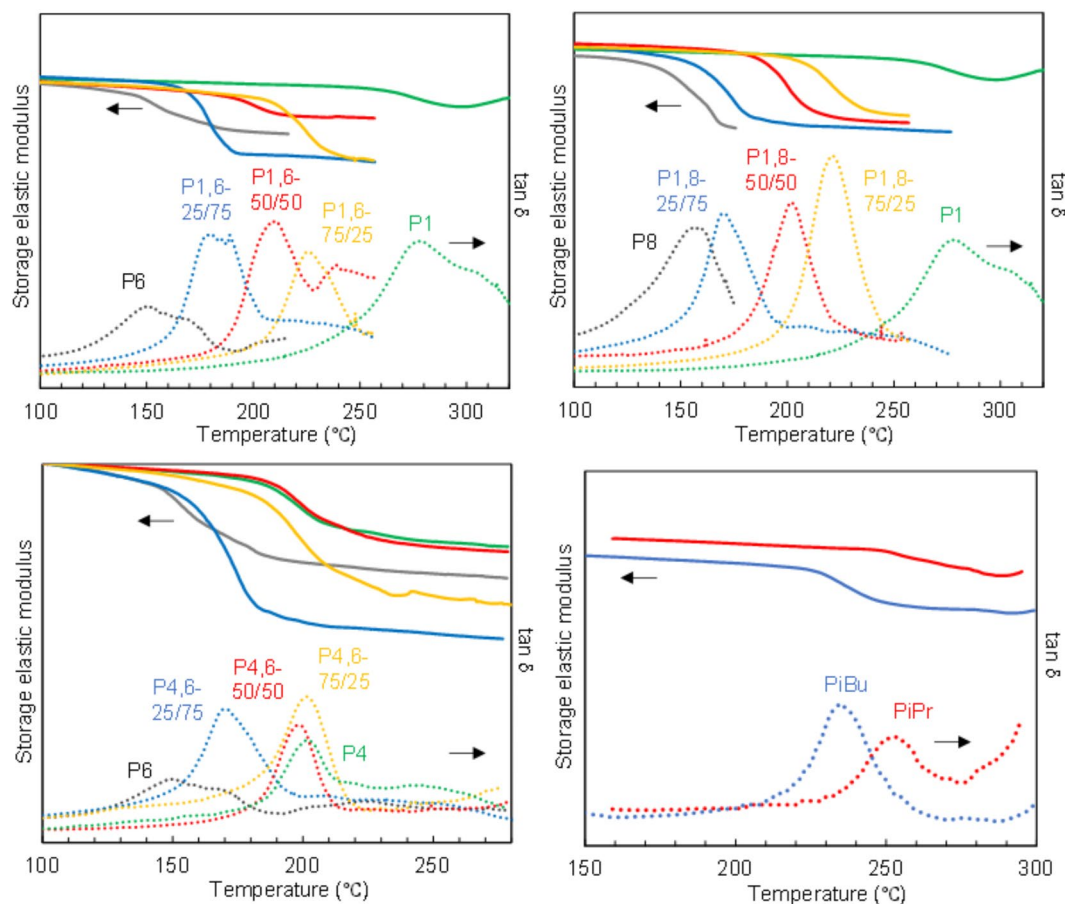


Fig. 5. DMA thermograms of (a) P16, (b) P18, (c) P46, and (d) branched DVAPAs.

was too hard to submit to tensile testing and P8 showed the lowest tensile strength of the specimens. P4 and P6 showed similar tensile strength even though their T_g values differed considerably (201 and 170 °C, respectively).

Regarding the co-PAs, there was a tendency for the tensile strength to increase with the content of shorter side chains. The mechanical properties of the PAs were modulated by the side-chain structure and composition ratio. In particular, in the case of P16-75/25, by combining 75% of Me-DVA with 25% of a longer-chain Hex-DVA component, mechanical strength and T_g increased remarkably, and mechanical strength was maintained compared with those of P6. In the case of P18-75/25, both mechanical strength and T_g were much higher than those of P8, as shown in Fig. 8. In both types of co-PAs, elongation at break values increased and Young's modulus decreased slightly compared with those of P6 or P8 long-chain PAs. In other words, P1 was too brittle and hard but adding a longer-chain component increased its processability while maintaining high thermal stability and mechanical strength. In the case of P46 PAs, there was no clear dependence of side-chain composition ratio on mechanical strength, which is probably because P4 and P6 had similar mechanical properties.

The branched PA PiPr displayed a mechanical strength of 63.8 MPa, Young's modulus of 1.32 GPa, and the highest T_g among the PAs except for that of P1. Overall, the branched side-chain structure contributed to the improved mechanical strength compared with that of PAs with linear side chains.

Focusing on PiPr, P6, P16-75/25, P4, and P46-25/75, these PAs exhibited high tensile strength of approximately 60 MPa, which exceeds that of the other PAs. In contrast, T_g of these PAs varied over the wide range from 170 to 253 °C. The branched PA, PiPr, exhibited the highest T_g of 253 °C, a tensile strength of 63 MPa, and the highest Young's modulus of 1.32 GPa. The co-PA P16-75/25 showed a high T_g of 225 °C while maintaining similar mechanical properties to those of P6 with a T_g of 170 °C. These results mean that it is possible to control the thermal stability of PAs according to the required processing temperature and purpose while maintaining mechanical strength. Similar phenomena have been observed in the case of polysaccharide ester derivatives with branched side-chains which exhibited extraordinary higher T_g and T_m compared to the esters with linear side-chains, and the branched esters also exhibited the highest Young's modulus^{29–32}. We need to note that the molecular weights of PAs are different, as shown in Table 1. Therefore, thermal and mechanical properties might be affected by molecular weight to some extent. However, the difference in the molecular weights of the compared PAs is not significant (ca. $9\text{--}13 \times 10^4$ g/mol). We consider that the result that the PA with the branched side-chains had extraordinary high T_g might be mainly caused by molecular mobility limitation owing to the branched side-chains.

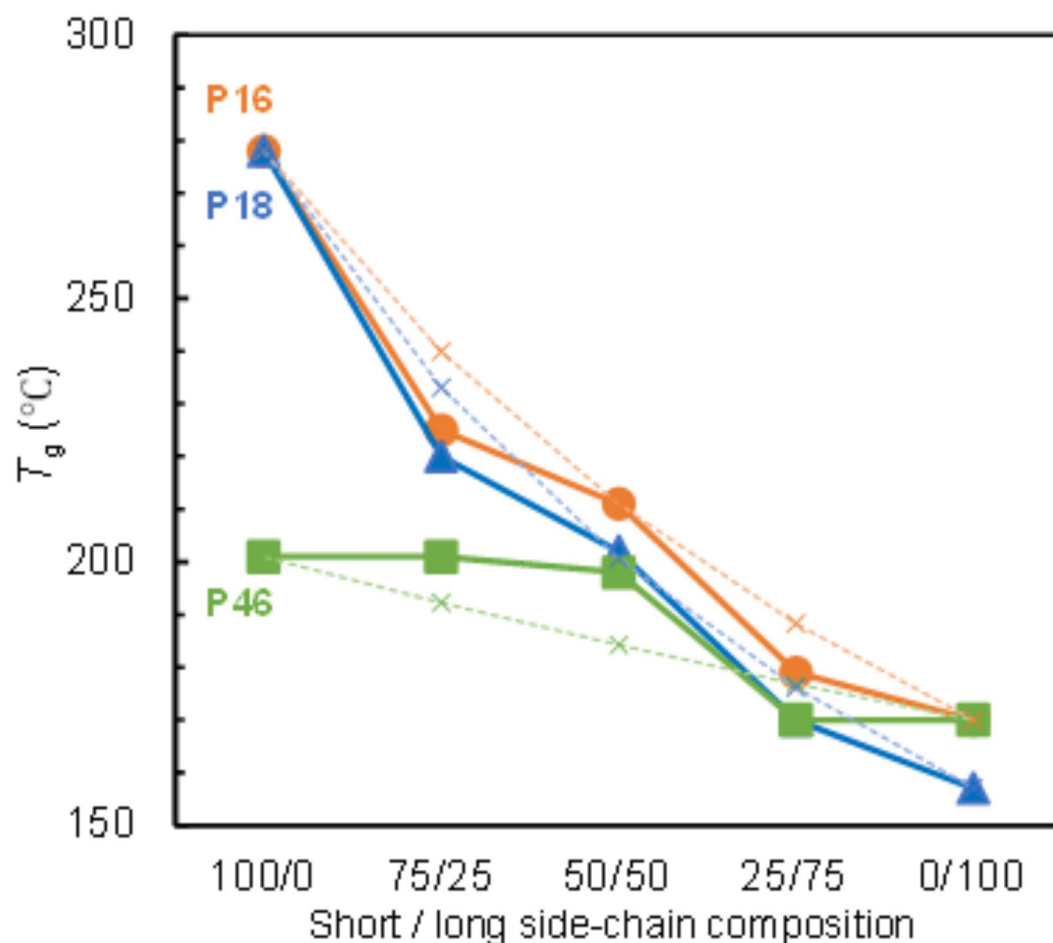


Fig. 6. The T_g plots against side-chain composition. Solid: Experimental value determined by DMA. Cross: Theoretical value calculated based on the Fox equation.

Conclusions

R-DVA with branched or linear side chains were synthesized from methyl-VA. DVA-based aromatic PAs with branched side chains and co-PAs with different combinations of linear side chains were synthesized by the polycondensation of R-DVA with appropriate side chains. The DVA PAs were amorphous with a T_d of 380 °C, illustrating their high thermal stability. The T_g values of the PAs depended on the side-chain structure and composition ratio. The branched PAs with isopropyl side chains exhibited the highest T_g of the PAs of 253 °C. Thermo-pressed films of the DVA PAs were prepared. Tensile testing of the thermo-pressed films revealed that the mechanical properties of the PAs depended on the side-chain structure and composition ratio. The tensile strength of the PAs increased with the composition ratio of shorter side chains. The PA with branched side chains, PiPr, exhibited the highest T_g of 253 °C and highest tensile strength of 63 MPa of the specimens. The thermal and mechanical properties of DVA PAs depend on side-chain structure and composition ratio, providing a pathway to access biopolymers with desired properties.

Materials and methods

Materials

Methyl vanillate (Methyl-VA) was purchased from Tokyo Kasei Co., Ltd. (Tokyo, Japan). *N*-Methyl-2-pyrrolidinone (NMP) and triphenyl phosphite (TPP) were purchased from Wako (Tokyo, Japan). All other reagents were obtained commercially and used as received. Dimethyl divanillate (dimethyl-DVA), dimethyl dialkoxydivanillate (dimethyl-R-DVA), and dialkoxydivanillic acid (R-DVA) were synthesized following reported protocols²⁴; note that R represents dialkoxy side chains (R = methyl, butyl, hexyl, octyl, *i*-propyl (iPr), or *i*-butyl (iBu)). 4,4-Methylenedianiline (MDA) was purchased from Wako Pure Chemical Industries, Ltd. (Tokyo, Japan) and used as received.

Synthesis of PAs with alkyl side chains

PAs were synthesized following the method described in our previous article²⁴. Samples are denoted using the number of carbon atoms ($n=1, 4, 6, 8$) and ratio of precursors with different side chains. A representative synthesis of P46-25/75 is as follows: butyl-DVA (0.112 g, 0.25 mol%), hexyl-DVA (0.376 g, 0.75 mol%), and LiCl



Fig. 7. Photographs of thermo-pressed films of DVA PAs.

(0.157 g) were dissolved in NMP (2.3 mL). An equimolar amount of MDA (0.57 mg, 1.0 mol%) together with pyridine (0.6 mL) and TPP (0.3 mL) were added to the flask, which was then filled with nitrogen and heated overnight at 130 °C. The following day, the solution was poured into methanol, and the precipitated product was washed with methanol followed by deionized water. Finally, the product was dried overnight *in vacuo* at 100 °C. P46-25/75 was obtained as a gray solid (0.379 g, 77.7%). All PAs were synthesized in this manner with different combinations of monomers and are denoted according to the carbon number of their side chain and composition ratio. Representative NMR assignment of P46-25/75 is as follows: $^1\text{H-NMR}$ (DMAO- d_6): 0.68, 0.97, 1.03, 1.32 (CH_2), 3.56, 3.8 ($\text{CH}_3\text{O-}$), 7.14, 7.58, 7.62 (Aromatic-H), 10.0 (NH). $^{13}\text{C-NMR}$ (DMAO- d_6): 13.8, 22.0, 24.9, 29.4, 30.9 (CH_2), 55.9 ($\text{CH}_3\text{O-}$), 72.3 ($-\text{CH}_2\text{O-}$), 111.7, 120.6, 122.4, 129.2, 128.7, 129.1, 131.8, 136.6, 137.1, 148.5, 149.0, 152.2 (Aromatic-C), 164.9 (C=O).

Synthesis of PAs with branched side chains

PAs were synthesized following the method described in our previous article²⁴. Samples are denoted as PAR according to the side chain R (R = iPr, iBu). A representative synthesis of PA with iPr side chains (PiPr) (R = iPr, $\text{CH}(\text{CH}_3)_2$) is as follows: iPr-DVA (1.2 g) and LiCl (0.40 g) were dissolved in NMP (6.0 mL). An equimolar amount of MDA (0.57 mg) together with pyridine (1.5 mL) and TPP (1.5 mL) were added to the flask, which was then filled with nitrogen and heated overnight at 130 °C. The following day, the product was precipitated in methanol and washed with methanol followed by deionized water. Finally, the product was dried overnight *in vacuo* at 100 °C. PiPr was obtained as a gray solid (1.5 g, 84.6%). PiBu (R = iBu, $\text{C}(\text{CH}_3)_3$) was synthesized in the same manner using iBu-DVA. Representative NMR assignment of PiPr is as follows: $^1\text{H-NMR}$ (DMAO- d_6): 0.92 (CH_3), 3.87 ($\text{CH}_3\text{O-}$), 4.18 (CH), 7.16, 7.60, 7.63 (Aromatic-H), 10.0 (NH). $^{13}\text{C-NMR}$ (DMAO- d_6): 22.3 (CH_3), 56.0 ($\text{CH}_3\text{O-}$), 74.6 (CHO-), 111.4, 120.6, 122.6, 129.2, 128.7, 132.3, 136.7, 137.1, 147.3, 152.3 (Aromatic-C), 164.4 (C=O).

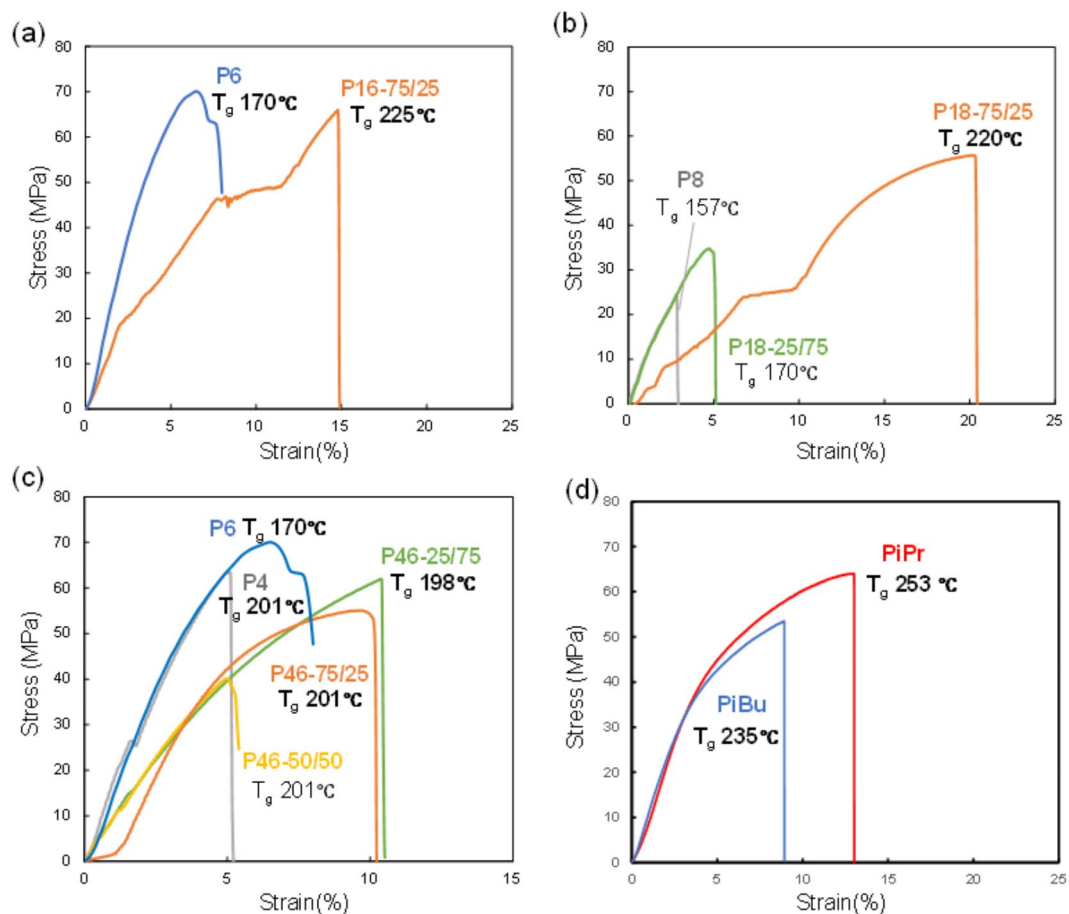


Fig. 8. Strain-stress curves of the thermo-pressed films of (a) P16, (b) P18, (c) P46, and (d) branched DVAPAs.

Polyamide	T_g (°C)	Tensile Strength (MPa)	Elongation at break (%)	Young's Modulus (GPa)
P1	278	-	-	-
P4	201	59.1 ± 8.3	9.0 ± 2.1	0.89 ± 0.11
P6	170	61.1 ± 14.9	9.4 ± 1.8	1.10 ± 0.27
P8	157	17.4 ± 5.1	2.3 ± 0.5	0.91 ± 0.29
P16-75/25	225	61.0 ± 4.6	13.8 ± 3.9	0.27 ± 0.08
P18-75/25	220	42.2 ± 10.5	20.3 ± 4.0	0.21 ± 0.05
P18-25/75	170	22.4 ± 9.3	8.6 ± 2.2	0.50 ± 0.30
P46-75/25	201	55.4 ± 10.3	11.6 ± 1.1	0.91 ± 0.11
P46-50/50	198	46.0 ± 5.0	6.0 ± 1.7	0.93 ± 0.07
P46-25/75	170	63.0 ± 2.1	12.3 ± 3.0	0.43 ± 0.15
PiPr	253	63.8 ± 2.5	11 ± 4	1.32 ± 0.11
PiBu	235	54.4 ± 3.1	8 ± 3	1.22 ± 0.24

Table 3. Mechanical properties of DVAPAs.

¹H NMR spectroscopy measurements

¹H and ¹³C nuclear magnetic resonance (NMR) spectra were obtained using an FT-NMR 500-MHz spectrometer (JEOL, JNM-A500, Tokyo, Japan) at room temperature, with deuterated chloroform-*d* or dimethylsulfoxide-*d*₆ as the solvent and tetramethylsilane as an internal standard.

Size-exclusion chromatography

Number- and weight-average molecular weight (M_n and M_w , respectively) and polydispersity (M_w/M_n) were estimated by size-exclusion chromatography (SEC; CBM-20A, DGU-20A_{3R}, LC-20AD, SIL-20AC, SPD-20A, CTO-20AC, RID-10A, FRC-10A; Shimadzu, Japan) in 1% LiCl/*N,N'*-dimethylacetamide (DMAc). Shodex

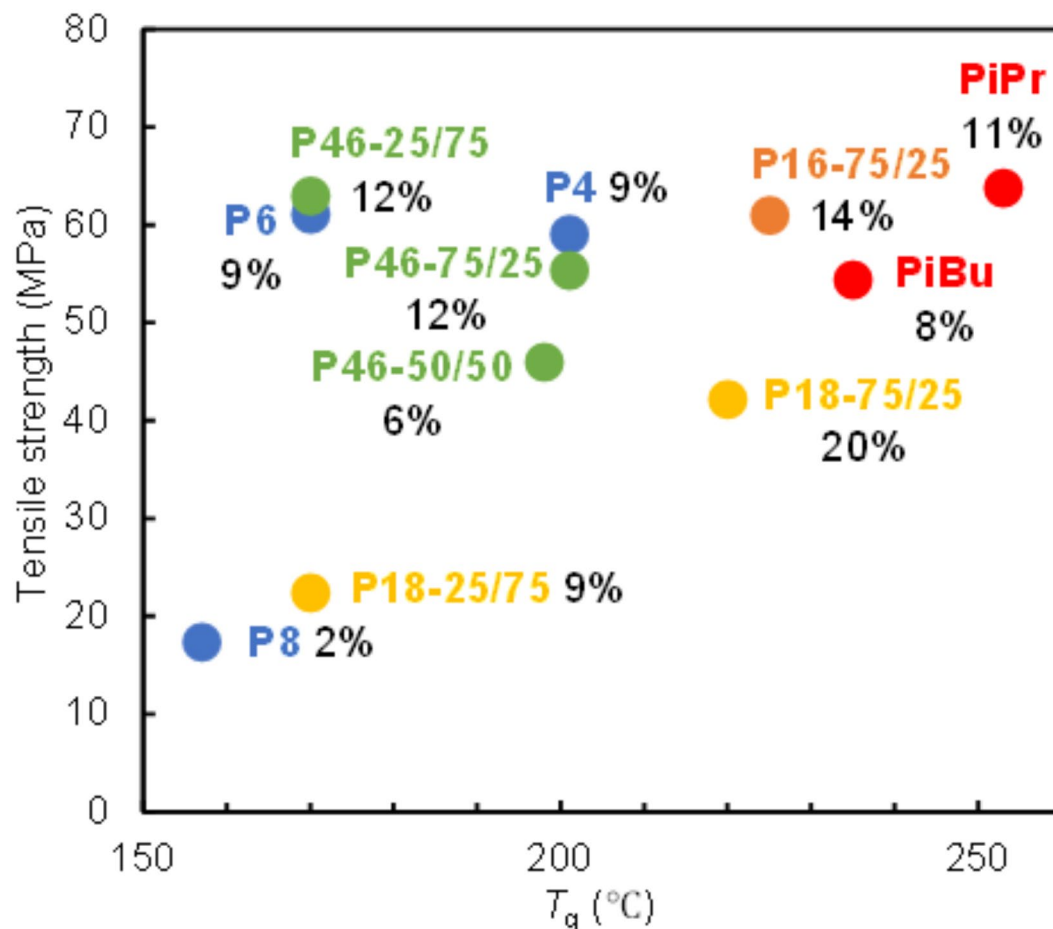


Fig. 9. Plots of tensile strength vs. T_g of the thermo-pressed films of polyamides with elongation at break values.

columns (KF-803 L, KF-806 L) were used at a flow rate of 0.6 mL/min. Polystyrene standards (Shodex) were used to construct a calibration curve.

Thermogravimetric analysis (TGA)

The thermal stability of the PA samples was tested using a thermogravimetric analyzer (TGA-50, Shimadzu, Japan) under nitrogen from 50 to 500 °C at a heating rate of 20 °C min⁻¹.

Dynamic mechanical analysis (DMA)

T_g of each polymer was measured on a dynamic mechanical analyzer (DMA 8000, Perkin-Elmer). The measurements were conducted by enclosing each powder sample in a material pocket, which was heated at a rate of 2 °C min⁻¹ from 100 °C to the temperature at which the tan δ peak for each sample was clearly observed.

Thermo-pressed films

The samples were placed between polytetrafluoroethylene sheets and pressed at 240 to 300 °C and 5 MPa using a Mini Test Press 10 (Toyoseiki, Japan). After heat-pressing, the films were quenched with water.

Tensile testing

The mechanical properties of the thermo-pressed films were measured with a universal tester (EZ-LX, Shimadzu, Japan) using a crosshead speed of 1 mm min⁻¹ and initial gauge length of 10 mm. Five specimens (20 × 3 mm) were used for each measurement and the data were averaged for each composition ratio.

Data availability

Spectroscopic data and thermal and mechanical analytical data are available on request.

Received: 14 November 2024; Accepted: 30 January 2025

Published online: 14 February 2025

References

1. Isikgor, F. H., Becer, C. R. & Lignocellulosic Biomass A sustainable platform for the production of Bio-based chemicals and polymers. *Polym. Chem.* **6**, 4497–4559 (2015).
2. Fache, M., Boutevin, B. & Caillol, S. Vanillin, a Key-Intermediate of Biobased polymers. *Eur. Polym. J.* **68**, 488–502 (2015).
3. Sousa, A. F. et al. Biobased polyesters and other polymers from 2,5-Furandicarboxylic acid: A tribute to Furan excellency. *Polym. Chem.* **6**, 5961–5983 (2015).
4. Vilela, C. et al. The quest for sustainable polyesters—insights into the future. *Polym. Chem.* **5**, 3119–3141 (2014).
5. Luo, K. J., Wang, Y., Yu, J. R., Zhu, J. & Hu, Z. M. Semi-bio-based aromatic polyamides from 2,5-Furandicarboxylic acid: Toward high-performance polymers from renewable resources. *RSC Adv.* **6**, 87013–87020 (2016).
6. Gomes, M., Gandini, A., Silvestre, A. J. D. & Reis, B. Synthesis and characterization of poly(2,5-Furan Dicarboxylate)S based on a variety of diols. *J. Polym. Sci. Part. A-Polym. Chem.* **49**, 3759–3768 (2011).
7. Suvannasara, P. et al. Biobased polyimides from 4-aminocinnamic acid photodimer. *Macromolecules* **47**, 1586–1593 (2014).
8. Tateyama, S. et al. Ultrastrong, transparent polytruxillamides derived from microbial photodimers. *Macromolecules* **49**, 3336–3342 (2016).
9. Ali, M. A., Shimosegawa, H., Nag, A., Takada, K. & Kaneko, T. Synthesis of thermotropic polybenzoxazole using 3-Amino-4-Hydroxybenzoic acid. *J. Polym. Res.* **24**, 214 (2017).
10. Mialon, L., Vanderhenst, R., Pemba, A. G. & Miller, S. A. Polyalkylenehydroxybenzoates (Pahbs): Biorenewable aromatic/aliphatic polyesters from lignin. *Macromol. Rapid Commun.* **32**, 1386–1392 (2011).
11. Pang, C. C. et al. Renewable polyesters derived from 10-Undecenoic acid and vanillic acid with versatile properties. *Polym. Chem.* **5**, 2843–2853 (2014).
12. Sazanov, Y. N. et al. Polymeric materials derived from vanillic acid. *Russ. J. Appl. Chem.* **75**, 777–780 (2002).
13. Wilsens, C. et al. Processing and performance of aromatic-aliphatic thermotropic polyesters based on vanillic acid. *Polymer* **60**, 198–206 (2015).
14. Bock, L. H. & Anderson, J. K. Linear polyesters derived from vanillic acid. *J. Polym. Sci.* **17**, 553–558 (1955).
15. Mialon, L., Pemba, A. G. & Miller, S. A. Biorenewable polyethylene terephthalate mimics derived from lignin and acetic acid. *Green Chem.* **12**, 1704–1706 (2010).
16. Llevot, A., Grau, E., Carlotti, S., Grelier, S. & Cramail, H. Admet polymerization of bio-based biphenyl compounds. *Polym. Chem.* **6**, 7693–7700 (2015).
17. Llevot, A., Grau, E., Carlotti, S., Greliera, S. & Cramail, H. Renewable (Semi)aromatic polyesters from symmetrical vanillin-based dimers. *Polym. Chem.* **6**, 6058–6066 (2015).
18. Savonnet, E. et al. Divanillin-based aromatic amines: Synthesis and use as curing agents for fully vanillin-based epoxy thermosets. *Front. Chem.*, **7**, (2019).
19. Enomoto, Y. & Iwata, T. Synthesis of biphenyl polyesters derived from divanillic acid, and their thermal and mechanical properties. *Polymer* **193**, 122330 (2020).
20. Zhang, Y. F., Enomoto, Y. & Iwata, T. Synthesis and characterization of biphenyl polyesters derived from divanillic acid and cyclic diols. *Polymer*, **203**, (2020).
21. Zhang, Y. F., Enomoto, Y. & Iwata, T. Synthesis of homo- and copolyesters containing divanillic acid, 1,4-Cyclohexanedimethanol, and alkanediols and their thermal and mechanical properties. *Polym. Degrad. Stab.* **192**, 109706 (2021).
22. Fujieda, K., Enomoto, Y., Huang, Q. Y. & Iwata, T. Synthesis and enzymatic biodegradation of co-polyesters consisting of divanillic acid with free hydroxyl groups. *Polymer*, **268**, (2023).
23. Fujieda, K., Enomoto, Y., Zhang, Y. F. & Iwata, T. Synthesis and characterization of Novel potentially biodegradable aromatic polyesters consisting of divanillic acids with free phenolic hydroxyl groups. *Polymer* **257**, 125241 (2022).
24. Yagura, K., Zhang, Y. F., Enomoto, Y. & Iwata, T. Synthesis of highly thermally stable divanillic acid-derived polyamides and their mechanical properties. *Polymer* **228**, 123907 (2021).
25. Yagura, K., Enomoto, Y. & Iwata, T. Synthesis of fully divanillic acid-based aromatic polyamides and their thermal and mechanical properties. *Polymer* **256**, 125222 (2022).
26. Enomoto, Y. & Iwata, T. Synthesis and characterization of bio-based Aromatic polyketones and polyetherketones derived from divanillic acid. *Eur. Polymer J.* **154**, 110526 (2021).
27. Zhang, Y. F., Yukiko, E. & Tadahisa, I. Bio-based vitrimers from divanillic acid and epoxidized soybean oil. *Rsc Sustain.*, **1**, 543–53 (2023).
28. Danjo, T., Enomoto-Rogers, Y., Takemura, A. & Iwata, T. Syntheses and properties of glucomannan acetate butyrate mixed esters. *Polym. Degrad. Stab.* **109**, 373–378 (2014).
29. Zhai, W., Danjo, T. & Iwata, T. Synthesis and physical properties of Curdlan branched ester derivatives. *J. Polym. Res.* **25**, 181 (2017).
30. Zhai, W. & Iwata, T. Synthesis and properties of curdlan branched and linear mixed ester derivatives. *Polym. Degrad. Stab.* **161**, 50–56 (2019).
31. Fukata, Y., Kimura, S. & Iwata, T. Synthesis of A-1,3-Glucan branched ester derivatives with excellent thermal stability and thermoplasticity. *Polym. Degrad. Stab.* **177**, 109130 (2020).
32. Fukata, Y., Kimura, S. & Iwata, T. Synthesis and properties of A-1,3-Glucan with branched and Linear mixed ester side chains. *Acs Appl. Polym. Mater.* **3**, 418–425 (2021).
33. Zi, Y. et al. High-temperature-Induced shape memory copolyimide. *Polymers* **13**, 3222 (2021).
34. Brostow, W., Chiu, R., Kalogeras, I. M. & Vassilikou-Dova, A. Prediction of glass transition temperatures: Binary blends and copolymers. *Mater. Lett.* **62**, 3152–3155 (2008).
35. Fox, T. G. *Bull. Am. Phys. Soc.*, **1** 123 (1956).

Acknowledgements

We thank Natasha Lundin, PhD, from Edanz (<https://jp.edanz.com/ac>) for editing a draft of this manuscript.

Author contributions

Yukiko Enomoto: Investigation, conceptualization, writing-original draft preparation, supervision, funding acquisition, Yuto Amanokura: Investigation, Kazuma Yagura: Investigation, Tadahisa Iwata: supervision and reviewing.

Declarations

Competing interests

The authors declare no competing interests.

Additional information

Correspondence and requests for materials should be addressed to Y.E.

Reprints and permissions information is available at www.nature.com/reprints.

Publisher's note Springer Nature remains neutral with regard to jurisdictional claims in published maps and institutional affiliations.

Open Access This article is licensed under a Creative Commons Attribution-NonCommercial-NoDerivatives 4.0 International License, which permits any non-commercial use, sharing, distribution and reproduction in any medium or format, as long as you give appropriate credit to the original author(s) and the source, provide a link to the Creative Commons licence, and indicate if you modified the licensed material. You do not have permission under this licence to share adapted material derived from this article or parts of it. The images or other third party material in this article are included in the article's Creative Commons licence, unless indicated otherwise in a credit line to the material. If material is not included in the article's Creative Commons licence and your intended use is not permitted by statutory regulation or exceeds the permitted use, you will need to obtain permission directly from the copyright holder. To view a copy of this licence, visit <http://creativecommons.org/licenses/by-nc-nd/4.0/>.

© The Author(s) 2025